SLAC-TN-10-011

Design and Implementation of a Thermal and Acoustic X-ray Detector to Measure the LCLS Beam Energy

Jennifer L. Loos
Office of Science, Science Undergraduate Laboratory Internship Program

San Jose State University, San Jose, CA

SLAC National Accelerator Laboratory
Menlo Park, California

August 14, 2009

Prepared in partial fulfillment of the requirement of the Office of Science, Department of Energy's Science Undergraduate Laboratory Internship under the direction of Joe Frisch in the Linac Coherent Light Source group of the SLAC National Accelerator Laboratory.

Participant: _____
Signature

Research Advisor: _____
Signature

Table of Contents

1 ABSTRACT

Design and Implementation of a Thermal and Acoustic X-ray Detector to Measure the LCLS Beam Energy. JENNIFER L. LOOS (San Jose State University, San Jose, CA 95192) JOE FRISCH (SLAC National Accelerator Laboratory, Menlo Park, CA 94025).

On April 11, 2009, first light was seen from LCLS. The present apparatus being used to measure the x-ray beam energy is the Total Energy Sensor which uses a suite of thermal sensors. Another device is needed to cross-check the energy measurements. This new diagnostic tool utilizes radiation acoustic phenomena to determine the x-ray beam energy. A target is hit by the x-rays from the beam, and a voltage is generated in two piezoelectric sensors attached to the target in response to the consequent deformation. Once the voltage is known, the power can be obtained. Thermal sensors will also be attached to the target for calibration purposes. Material selection and design were based on: durability, ultra-high vacuum compatibility, safety and thermal properties. The target material was also chosen for its acoustic properties which were determined from tests using a frequency generator and laser. Initial tests suggest the device will function as anticipated.

2 INTRODUCTION

In April of 2009, the LCLS became fully operational with an x-ray energy range from 800 eV to 8 keV and a pulse energy around 1 mJ. The present device being used to measure the x-ray beam energy is a Total Energy Sensor [1] which is comprised of a suite of thermal sensor arrays. A Yttrium Aluminum Garnet (YAG) crystal which is part of the Direct Imager [2] is also being used for calibration and imaging purposes. Because additional measurements are needed for comparison and greater precision, the Thermal and Acoustic X-ray Detector will serve as a complementary diagnostic tool in determining the beam energy using acoustic and thermal detectors along with a YAG screen. Piezoelectric sensors will be used for the acoustic measurement and RTDs (resistive thermal detectors) will be used for the thermal measurement. This device will be placed in the beam dump area immediately after the electron beam dump in vacuum chamber ST0 upstream of the current FEE (front end enclosure) diagnostics.

The overall concept of the detector consists of a target being hit by the FEL light of the beam with the incoherent light being blocked by a shield. Attached to the target will be two piezoelectric sensors and two RTDs. This arrangement will rest on an aluminum bar which serves as both a platform for the target and shield as well as a heat sink. A clamp holding the shield in place will also function as a platform to which the YAG screen will be attached.

Although the piezoelectric effect has been applied to many areas of research, the use of acoustic devices for energy measurement is a relatively new technique. "Radiation acoustics is a field of physics in which sound phenomena arising under radiation interacting with matter are studied [3]." In this case, the shock wave from the x-ray beam will create vibrations in the target causing deformations in the target and the acoustic sensors which then generate a voltage in the latter. The power of the beam can then be determined from the measured voltage. "It was found that in tests with a fixed beam

and a target material in a fixed geometry, the probe output voltage was directly proportional to the peak power of incident beam [3]."

3 MATERIALS AND METHODS

Because this instrument will be placed in an ultra-high vacuum environment, careful consideration was given to the building materials that would be appropriate and most reliable. To insure safe and effective functioning of the device in the vacuum chamber, initial calculations were performed to estimate the amounts of ambient heating and the cooling time constants of all materials to be used. The thermal analysis of the materials to be used was done using the relationships:

$$P = A_1\sigma\,(T_1^4 - T_2^4) / [1/\varepsilon_1 + ((1-\varepsilon_2)\,A_1/\,\varepsilon_2\,A_2)]$$

where P is the radiative power transfer from a surface area A_1 with emissivity ε_1 at temperature T_1 to another surface area A_2 with emissivity ε_2 at temperature T_2, and σ is the Stefan-Boltzmann constant 5.67×10^{-8} W/m^{2}K [2], and h = (kA)/d where k is the thermal conductivity of the material, A is the surface area and d is the diameter. Then using: $\tau = C_v/h$, where C_v is the specific heat and h is the sum of the thermal conductivities of the materials divided by the thickness of the materials, the time constants were determined. (Table 1)

Platinum RTDs in a ceramic substrate were selected as ceramic materials are vacuum compatible and can be baked at high temperatures. Ceramic piezoelectric actuators were selected for their high Curie temperature and low out-gassing rate. For the shield, a layer of boron carbide (B_4C, another ceramic material) (2.5 x .5 x 1.24 cm) was chosen for the front with a thicker layer of tungsten (2.5 x 1.5 x 1.24 cm) backing it. The shield materials were chosen not only for their vacuum compatibility, but also for their ability to effectively block the spontaneous (incoherent) radiation from the beam allowing only the coherent 150 μm beam of x-rays to pass through a small collimator (3.25 mm hole) in the shield to the target. Because the target will absorb the x-ray beam, the very hard

materials B_4C (9.3 on Mohs hardness scale) and beryllium (5.5 on Mohs scale) were initially considered as the target material, with B_4C being the preferred material as beryllium is toxic. Another consideration in choosing the target material was to make sure it was one with a low atomic weight to ensure the material was not easily heated and had low x-ray absorption. Beryllium was considered as it gives a clear 'ringing' signal in response to interactions with ultra-sonic waves. Very little information was available about the acoustic properties of B_4C, so tests were performed to determine its viability as a target material.

To test the B_4C, two piezoelectric sensors (3 x 3 x 2 mm) were clamped on opposite sides of a small piece of B_4C (approximately 2.54 x 1.27 x .5 cm). Using a frequency generator, one of the piezos was driven, and the response of the second piezo was measured. From this, the resonances within the piezos were plotted, and a signal with a significant ringing time of about 200 μs was observed (Figure 1). The next test was to place the B_4C piece with the piezos casually clamped on to it in a laser beam at 1 mJ then 2 mJ to better simulate the x-ray beam. The response signal from the second piezo was about 100μV. This was lower than expected, and it was thought that perhaps the shape of the B_4C (and informality of the test) caused shearing modes that were not foreseen and weakened the signal. More formal tests were later performed to improve the signal.

Aluminum was selected for the heat sink and shield clamps for its efficient cooling properties and thus, relatively short time constant. (A short time constant is preferred so the temperature of the heat sink quickly reaches equilibrium with the outside and does not accumulate heat as the target is repeatedly interfacing with the beam). The aluminum bar will be attached to a translator positioned outside of the vacuum chamber that will move the bar up or down depending on which measurement (from the B_4C target or the YAG screen) is desired (Figure 3). A Thermionics Z-450 Series Translator was deemed best for this purpose for its stable motion. A close coupler will then be attached to the translator, and spherical octagon will be attached on top of the coupler. Feedthroughs will attach to the octagon. The wires from the RTDs and piezoelectric actuators will connect to the feedthroughs which

will then be connected to data acquisition electronics including a preamp (BJT Preamp SIM911) and an RTD monitor (SIM 923A).[1] The preamp was chosen for its especially low noise of 1.8 nV/√Hz which was calculated using: $N_{total} = V_n + I_nZ$ where V_n is the voltage noise, I_n is the current noise (1.2×10^{-12} A/√Hz) and Z is the impedance. The impedance was determined using the relationship: $Z = 1/[2\pi\omega C]$ where ω is the resonant frequency of the piezos and C is the capacitance. The total calculated noise was significantly less than the signal from the piezos, so this amplifier was considered a good choice.

4 RESULTS

For the second laser proof-of-concept test, to improve the signal, a cubic centimeter of B_4C was machined (1.25 x .8 x 1 cm) to be tested in the same fashion as the first laser test.[2] To improve the surface area contact between the piezos and the B_4C, the piezos were epoxied to the top and bottom of the cube. To further improve the signal, each piezo was also connected to four-to-one transformers and an amplifier set to a gain of 100. With the transformers, more symmetric B_4C shape and better experimental controls, much stronger signals were observed. Initially, the laser spot size was about the size of the target (~1 cm). With a laser energy of 1 mJ, and spot size of about 1 cm, the response signal was about 240 mV. (Figure 5) There was some increase in the signal when the laser beam spot size was minimized to approximately half the size of the surface of the target (268 mV). It was not expected that the spot size should make much difference in the signal response as long as the full diameter of the beam was in contact with the surface of the B_4C block. Because there was an increase in the signal as the result of the smaller spot size, it is thought that perhaps some of the beam was missing the target in the first test, but further tests are needed to better understand this.

---

[1] Preliminary visualizations of the device were done using Open Office Draw, and after further iterations of the overall design, technical drawings were completed using Solid Edge. (Figures 2, 3 and 4)

[2] Two such cubes of B_4C were machined: one for testing purposes, one for use in vacuum.

With the smaller spot size, tests were then done at a laser power of 1 mJ, 2 mJ and 2.6 mJ. At 1 mJ, the signal from channel 1, corresponding to one piezo, was about 268 mV, and from channel 2, corresponding to the other piezo, was about 236 mV (Figure 6). At 2 mJ of laser power, the signal was about 456 mV on channel 1 and 416 mV on channel 2 (Figure 7). Increasing the laser power from 1 to 2 mJ roughly doubled the signal, increasing it by about 180 mV. This fairly linear response was not seen when the power was increased from 2 to 2.6 mJ. At 2.6 mJ, the signal was 520 mV on channel 1 and 456 mV on channel 2 (Figure 8). (The signal only increased by about 55 mV). (Table 2, Figure 9) It was determined that further data would be required to obtain a more complete graph of response signal to beam power and better understand their relationship.

A third laser test was conducted to collect more comprehensive data and to possibly discover the cause of the non-linearity of the relationship between the laser beam power and the piezo response. For this test, the device was partially assembled, and the B_4C cube was epoxied to the aluminum bar. A low pass filter (50 Ω, 1.9 MHz) was placed before the amplifier for each channel. The addition of the filter caused an increase in the signal by a factor two (it is not fully understood why this is so). Measurements were taken at energies between .83 mJ and 2.67 mJ for gain settings of 100, 10 and 1. As in the second laser test, the roughly linear response from lower laser energy to around 2.3 mJ was observed. However, above 2.3 mJ, the non-linear relationship seen in the previous test occurred. It was thought that perhaps this was due to resonances within the amplifier, but this relationship was apparent even when there was no amplification (Figure 10, 11 and 12).

Another possible reason for the non-linearity is that there may be a saturation point for the piezo response at a certain laser energy, but further tests are required to study this. New tests will include further decreasing the spot size to better simulate the FEL beam to determine if the non-linearity is an issue of beam intensity; if the same relationship is observed with smaller and smaller spot sizes, it is likely due to a saturation point within the piezos.

5 DISCUSSION AND CONCLUSION

From preliminary tests, it appears that this device will be useful in determining the energy of the LCLS x-ray beam. Using results from the laser lab (once they are more comprehensive), it will be possible to obtain a value for the x-ray beam energy from the measured voltage induced in the piezoelectric sensors and the temperature change in the RTDs. By comparing these values with those of the Total Energy Sensor already in place, the power of the beam can be known with greater accuracy.

It is still not clear why there is not a linear relationship between the laser power and the piezo response at energies higher than ~2.3 mJ. The next tests done will be to determine whether or not the piezo electric sensors have a limiting voltage that is being exceeded at higher energies, or whether there are other material effects causing this relationship.

The materials selected for the device seem to be appropriate and effective. Design issues such as how to mount the various pieces to the aluminum bar to ensure stability and proper functioning in vacuum (leak prevention, etc.) have largely been remedied. However, final testing of the device will reveal any areas requiring further attention or improvement.

ACKNOWLEDGMENTS

Many thanks go to The Department of Energy Office of Science, SLAC National Accelerator Laboratory and the SULI program for providing this rewarding and very educational opportunity. Special thanks also go to my mentor Joe Frisch, Tonee Smith, Mark Petree, Phil Cutino, Dave Shelley and the machinists in Light Fabrication who lent their extensive expertise to this effort. Thanks also to fellow SULI student Greg Bentsen.

REFERENCES

[1] S. Friedrich et al, "Design of a bolometer for total-energy measurement of the linear coherent light source pulsed X-ray laser," *Nucl. Instr. Methods in Phys. Res. A* ,vol. 599, pp.772-774, 2006.

[2] Richard M. Bionta, "X-ray Transport Optics and Diagnostics Commissioning Report," *Lawrence Livermore National Laboratory Report* UCRL-PROC-207494, October 23, 2004.

[3] A.I. Kalinichenko, V.T. Lazurik, and I.I. Zalyubovsky, *The Physics and Technology of Particle and Photon Beams Volume 9: Introduction to Radiation Acoustics.* The Netherlands: Harwood Academic Publishers, 2001.

[4] Alexander Wu Chao, Ed. and Maury Tigner, Ed., *Handbook of Accelerator Physics and Engineering*. Singapore: World Scientific Publishing Co. Pte. Ltd., 1999.

[5] http://www.physikinstrumente.com/en/products/piezo_tutorial.php [Online]. [Accessed: June 2, 2009].

[6] James P. Wolfe, *Imaging Phonons: Acoustic Wave Propagation in Solids.* United Kingdom: Cambridge University Press, 1998.

[7] "Piezoelectricity," July 30, 2009. [Online]. Available: http://en.wikipedia.org/wiki/Piezoelectricity. [Accessed: June 3, 2009].

FIGURES AND TABLES

Boron Carbide (block)	
Specific Heat (J/kg*K)	9.500E+02
Density (kg/m^3)	2.520E+03
Molar Mass (g/mol)	5.500E+01
Size (cm)	1.000E+00
Thermal Conductivity (W/m*K)	3.500E+01
Thermal Expansion Coeff (um/m*K)	5.200E+00
Speed of Sound (m/s)	1.090E+04
Atten Length (um)	2.891E+00
Emissivity (1)	1.000E+00
Mass (kg)	2.520E-03
Target Specific Heat (J/K)	4.353E-02

Coefficients (h)	J. Loos	G. Bentsen
piezoelectric	4.950E-03	4.950E-03
wires	2.010E-04	2.010E-04
air	2.600E-04	1.600E-04
shield	5.640E-05	8.700E-05
container	2.600E-03	3.000E-03
Time constant for target (s)	295.95	293.1
Time constant for top piezo (s)	49.1	48.9
Time Constant for Aluminum Bar (s)	388.8	

Tungsten (material for shield)	
Min Mass Attenuation Coeff. (cm^2/g)	1.378E-01
Density (kg/m^3)	1.925E+04
Attenuation Length (cm)	3.770E-04
95% Length (cm)	1.131E-03
Specific Heat (J/kg*K)	1.300E+02
Molar Mass (g/mol)	1.838E+02
Emissivity (1)	4.000E-02
Shield Width (cm)	2.500E+00
Shield Height (cm)	2.000E+00
Shield Mass (g)	0.000E+00
Shield Specific Heat (J/K)	2.427E+01

Piezo	
Piezo Thermal Conductivity (W/m*K)	1.100E+00
Piezo Thickness (mm)	2.000E+00
Piezo Deformation Coeff (pm/V)	4.000E+02
Piezo Width (mm)	3.000E+00
Piezo Capacitance (C/V)	2.500E-08

Table 1: Heat and time constant calculations. Data calculated and compiled by G. Bentsen and J. Loos.

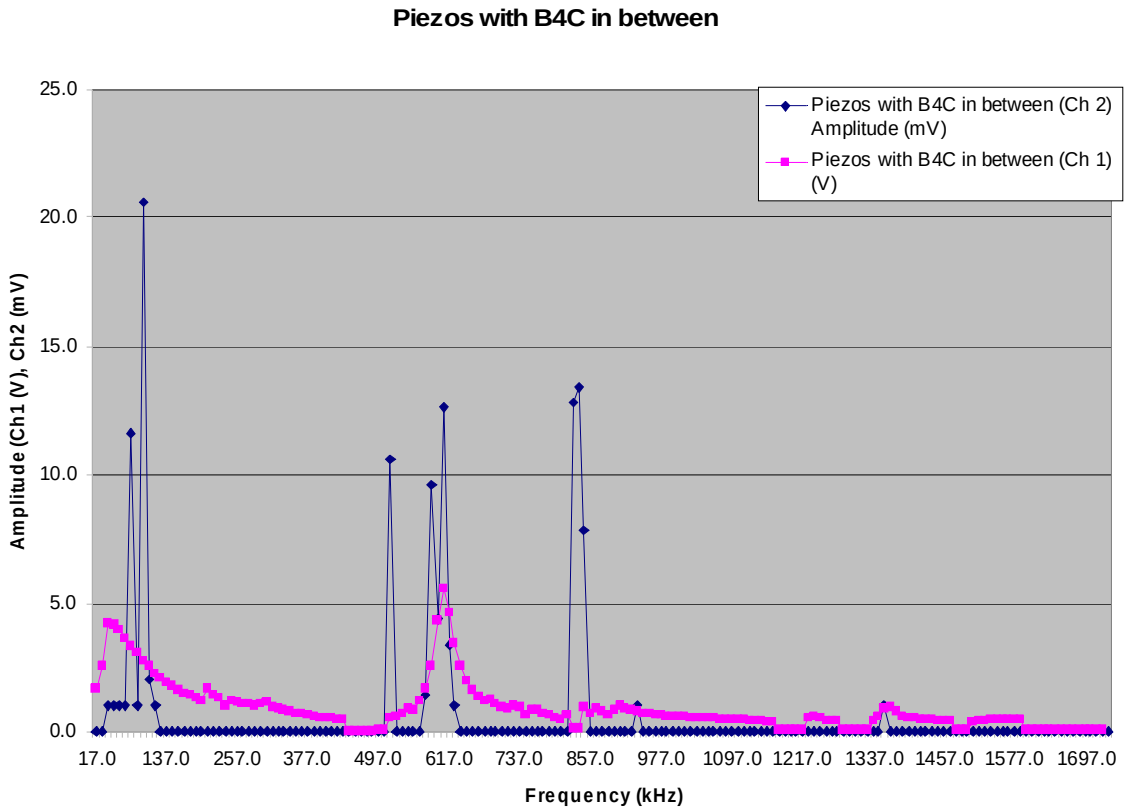

Figure 1: A signal is seen from an initial test of an irregularly-shaped piece of B_4C using a frequency generator. Ch 1 (pink) is the driving signal in volts, Ch 2 (blue) is the response signal from the second piezo in mV.

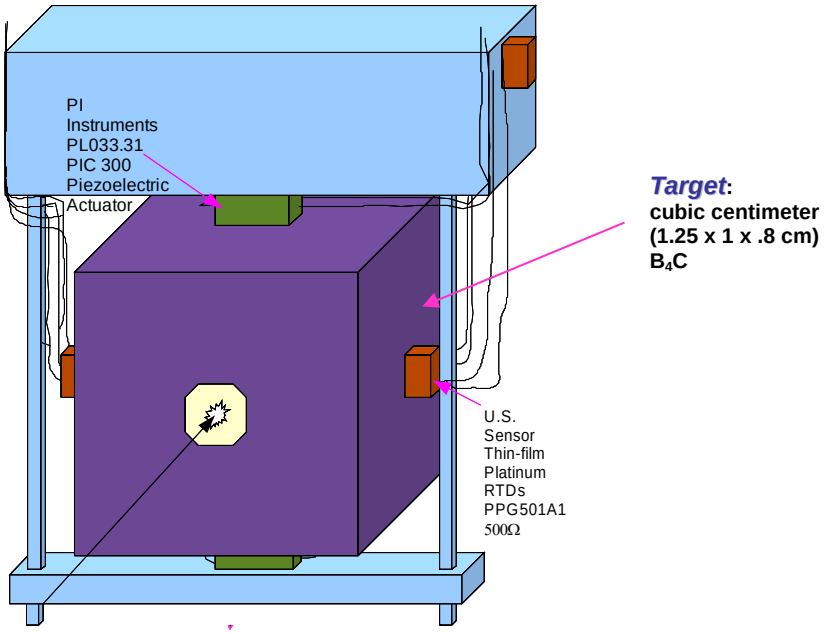

Figure 2: This is an early conceptual drawing of target with piezoelectric sensors and RTDs (J. Loos, June 2009).

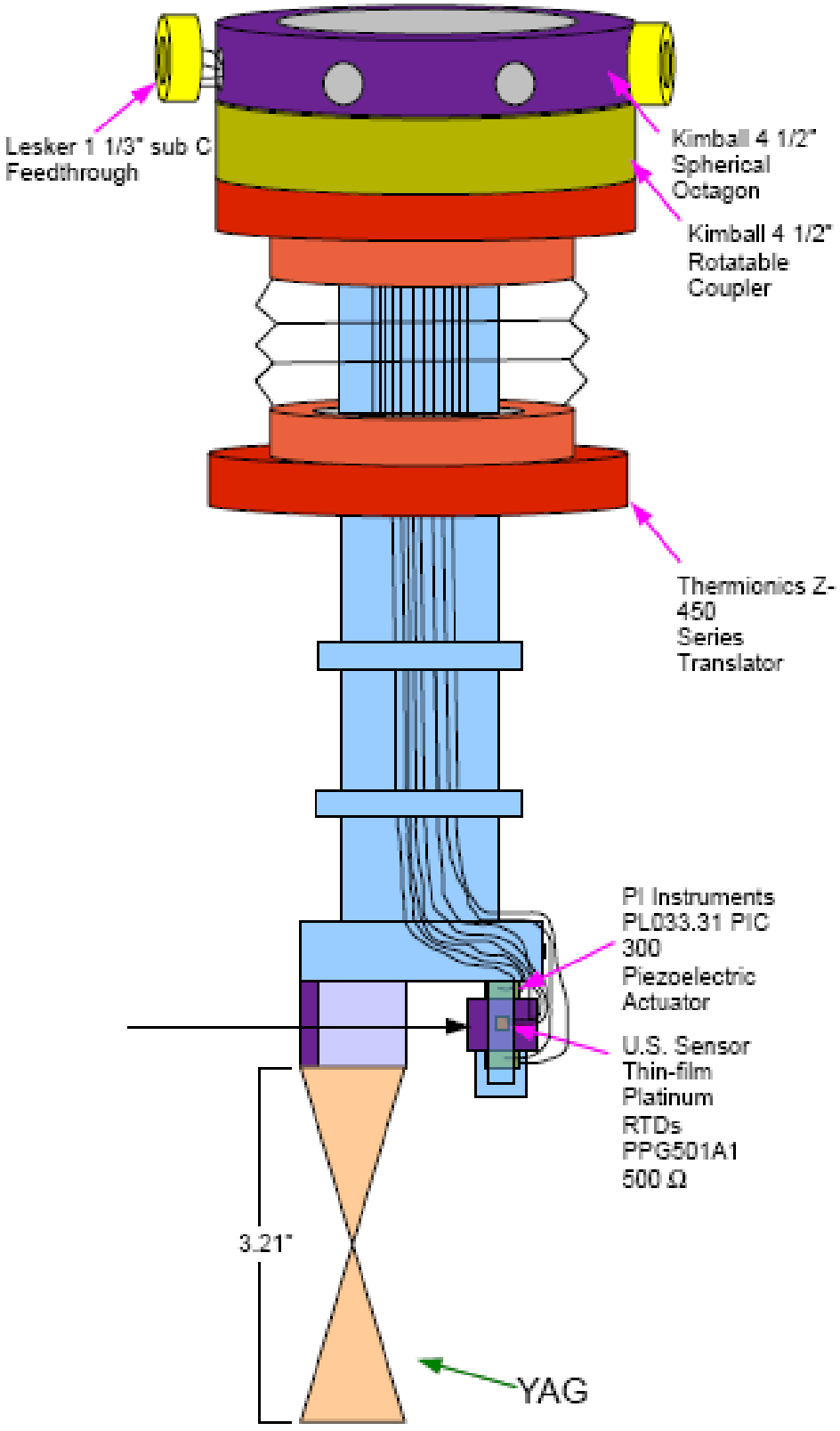

Figure 3: This is an early conceptual drawing for the device created in Open Office Draw (J. Loos, June 2009). In the final design, 100Ω RTDs and a non-rotatable coupler were chosen.

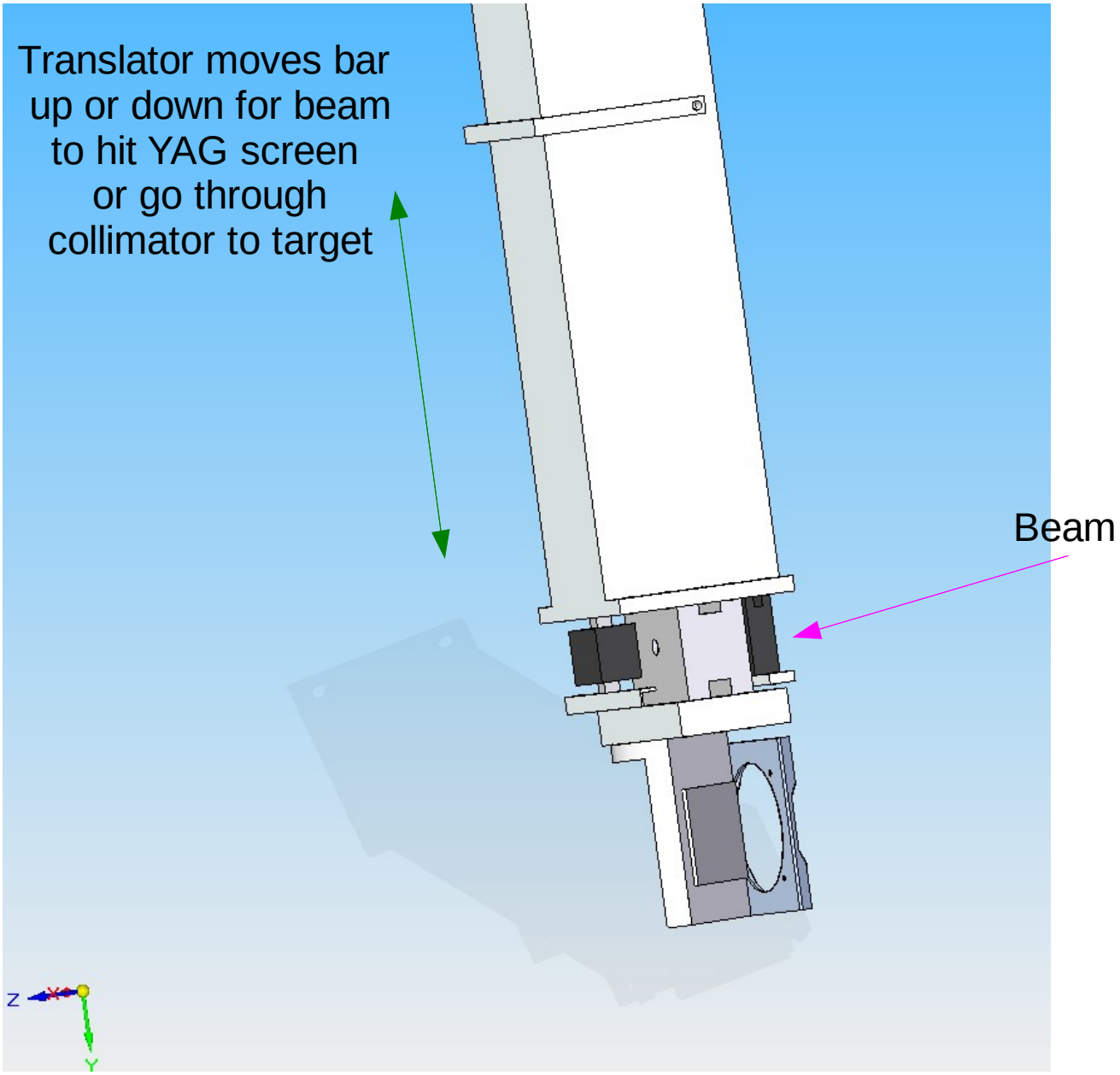

Figure 4: This is the lower half of the assembly with the B_4C cube and clamp, tungsten and B_4C shielding with clamps, YAG assembly, aluminum bar heat sink and wire clamp. (J. Loos, July 2009, Solid Edge).

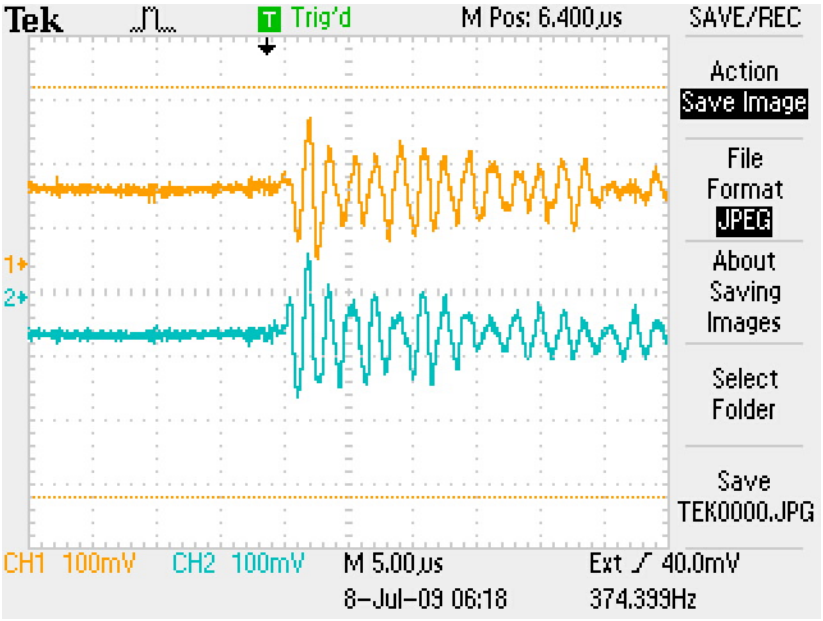

Figure 5: Second laser test with cubic centimeter of B4C, beam energy at 1 mJ, spot size about 1 cm, amplifier x100, signal (ch 1) of about 240 mV.

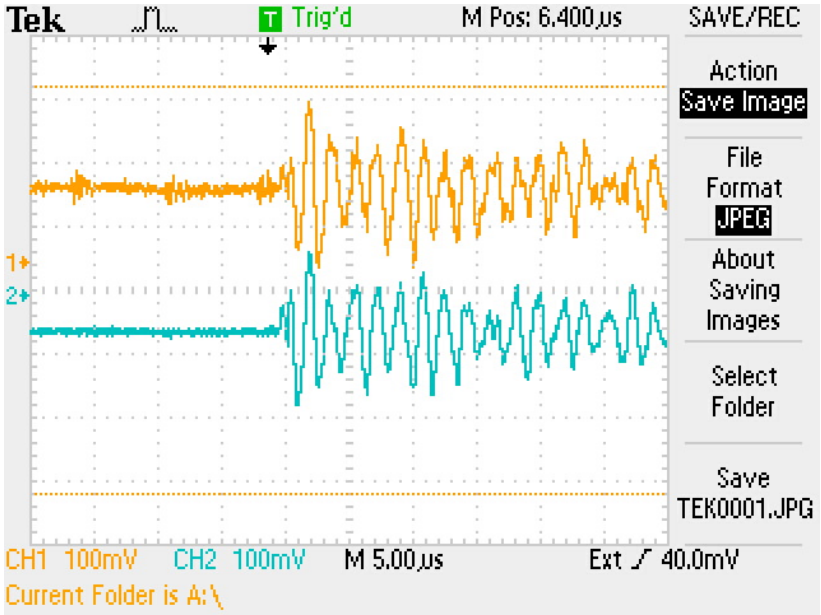

Figure 6: Second laser test with cubic centimeter of B4C, beam energy at ~1 mJ, spot size about .5 cm, amplifier x100, signal (ch 1) of about 268 mV, (ch 2) of about 236 mV.

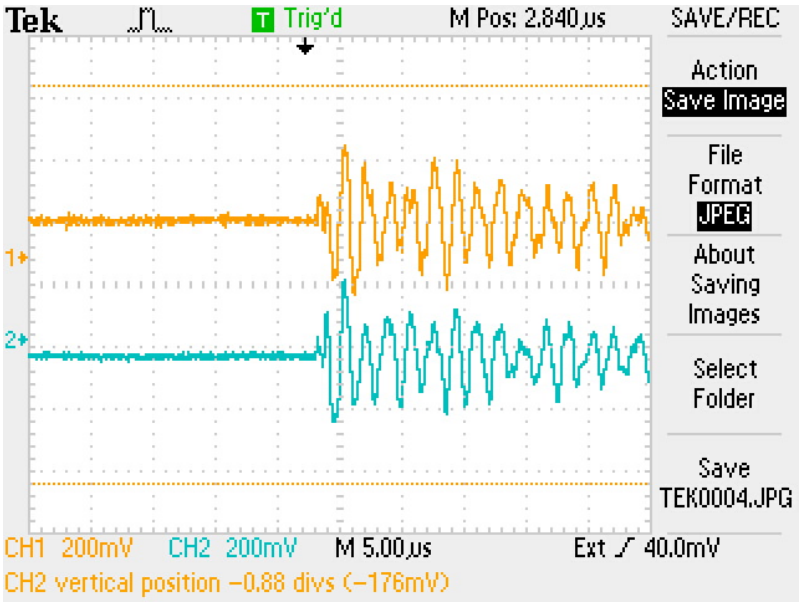

Figure 7: Second laser test with cubic centimeter of B4C, beam energy at ~2 mJ, spot size about .5 cm, amplifier x100, signal (ch 1) of about 456 mV, (ch 2) 416 mV.

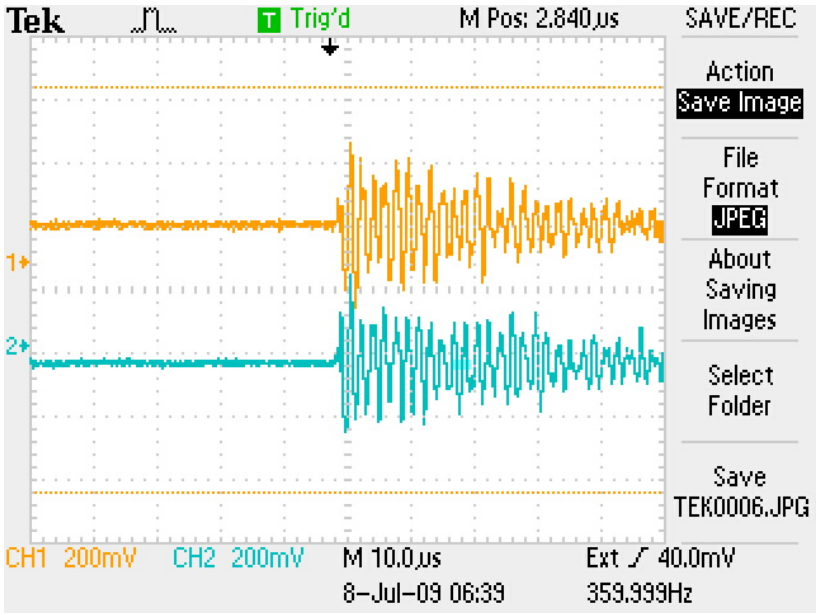

Figure 8: Beam energy at ~2.6 mJ, spot size about .5 cm, amplifier x100, signal (ch 1) of about 520 mV, (ch 2) 456 mV.

Laser Power (mJ)	Spot size (cm)	Channel 1 (mV)	Channel 2 (mV)
1	~ 1	240	220
1	~.5	268	236
2	~.5	456	416
2.6	~.5	520	456

Table 2: Measurements of the response signal (mV) from the piezos as a result of the laser power (mJ) and spot size, second laser test.

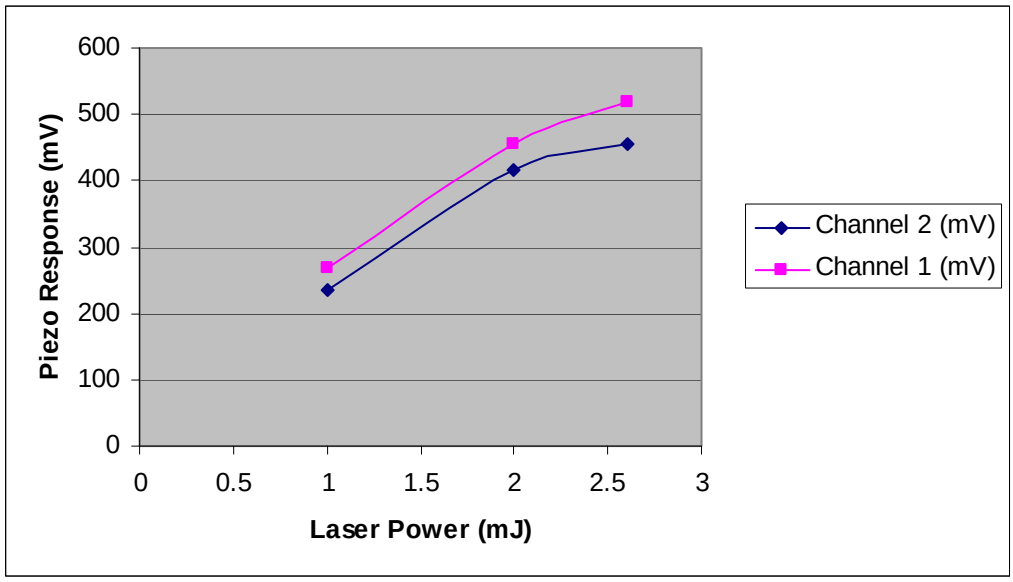

Figure 9: Plot of laser power versus the piezo response showing a non-linear relationship, second laser test.

Laser Power	Channel 1 (x100)	Channel 2 (x100)	Channel 1 (x10)	Channel 2 (x10)	**Channel 1 (x1)**	**Channel 2 (x1)**
(mJ)	(mV)	(mV)	(mV)	(mV)	(mV)	(mV)
2.67	800.1	811.6	91.3	79.2	8.86	7.74
2.5			87.2	75.8	8.75	7.6
2.58	800.8	805.2	90.42	78.18		
2.33	787.1	741.4	81.9	70.94	8.18	7.11
2.17			77.3	66.2		
2	728.3	659.3	73.01	63.01		
1.67	629.6	551.8	62.3	54.07		
1.33	512.1	444.8	50.3	43.5		
1	390.4	337.1	38.51	33.4		
0.83	319.2	281.1	32.02	27.74		

Table 3: Third laser test data.

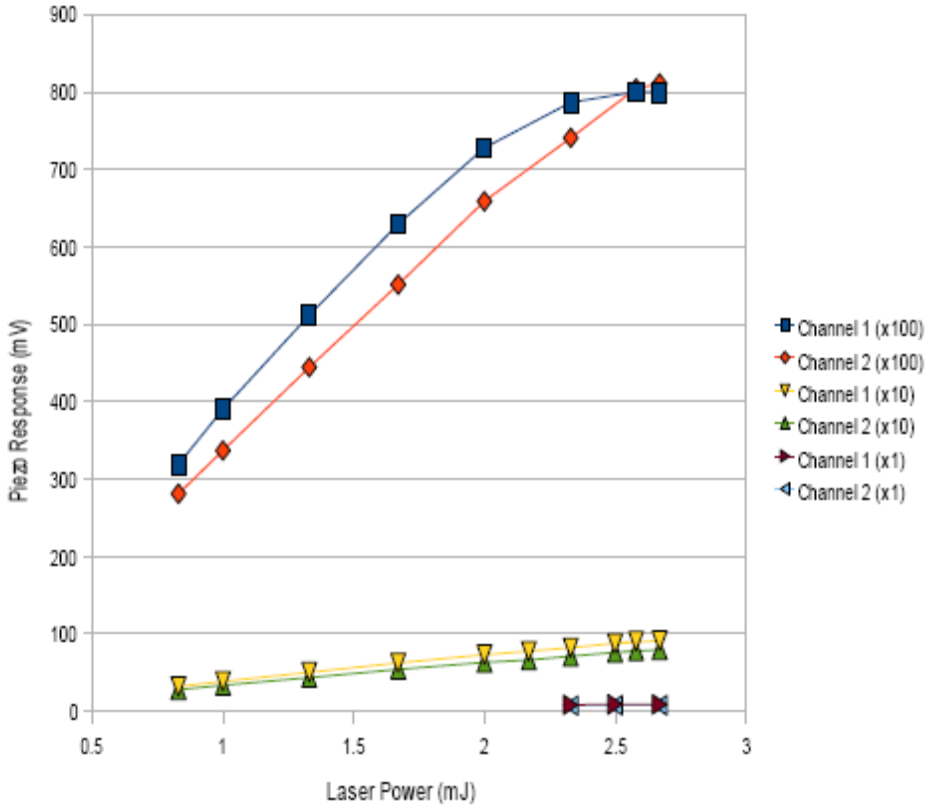

[Figure 10] Third laser test at gain of 100, 10 and 1.

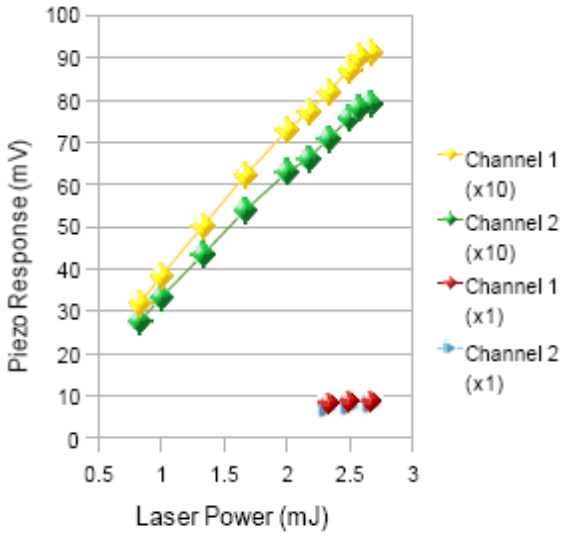

[Figure 11] Third laser test at gain of 10 and 1.

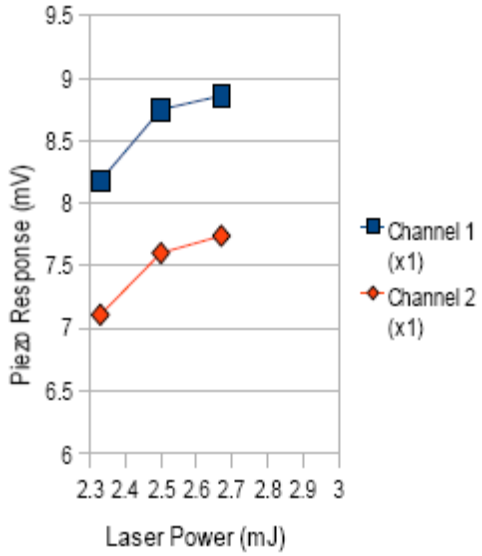

[Figure 12] Third laser test, no amplification.

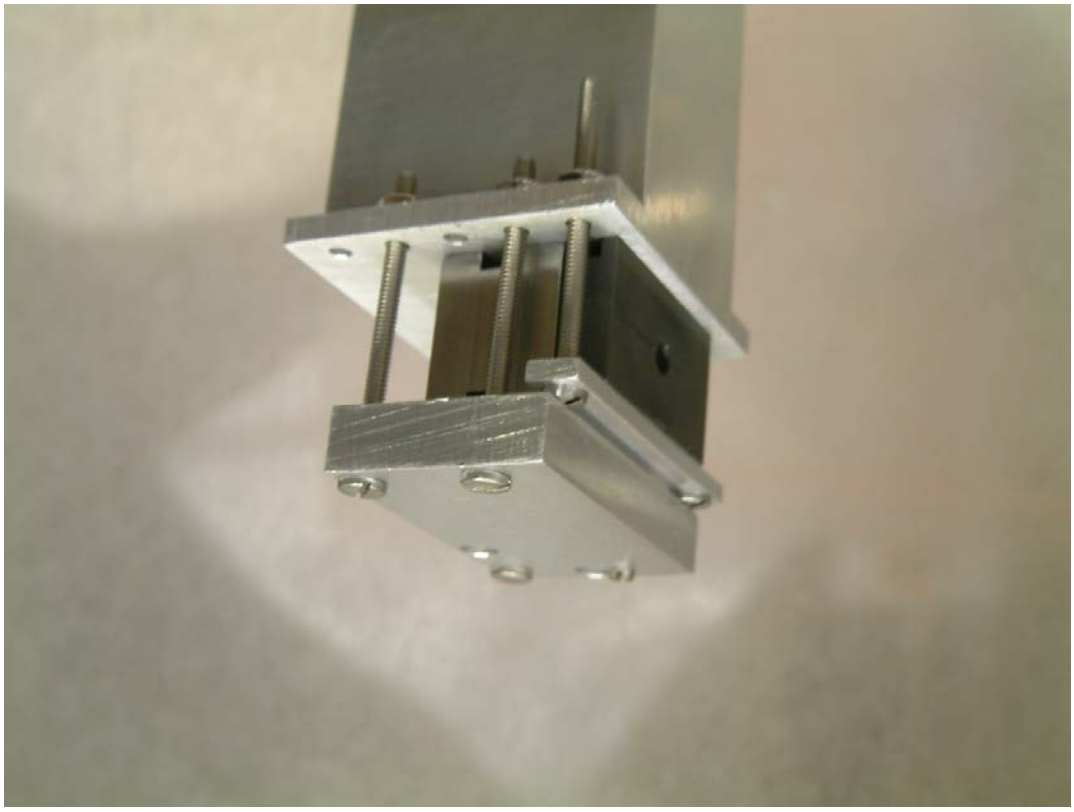

[Figure 13] Partial assembly of detector with shielding and aluminum bar.

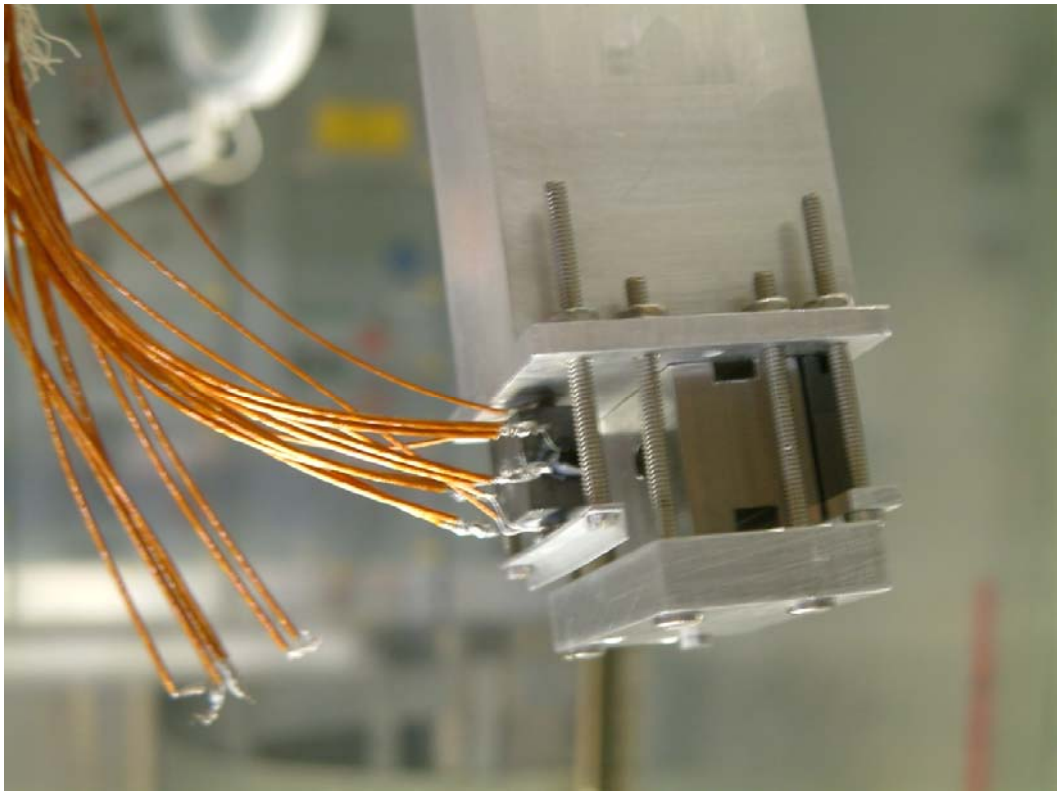

[Figure 14] Partial assembly of detector with shielding, B_4C cube, RTDs, piezos and aluminum bar.